Available online at www.sciencedirect.com
ScienceDirect
Journal of Computational Physics 219 (2006) 477–488
JOURNAL OF COMPUTATIONAL PHYSICS
www.elsevier.com/locate/jcp

Short note

# Spectral convergence of the Hermite basis function solution of the Vlasov equation: The free-streaming term

Livio Gibelli [a], Bernie D. Shizgal [a,b,*]

[a] *Department of Chemistry, University of British Columbia, 2036 Main Mall, Vancouver, BC, Canada V6T 1Z1*
[b] *Institute of Space and Astronautical Science (ISAS), Japan Space Exploration Agency (JAXA), 3-1-1 Yoshinodai, Sagamihara, Kanagawa 229-8510, Japan*

Received 10 January 2006; received in revised form 5 June 2006; accepted 9 June 2006
Available online 9 August 2006

*Keywords:* Vlasov equation; Spectral methods; Hermite basis functions; Filamentation; Recurrence

## 1. Introduction

The theoretical description of the mechanisms for the energization of ions in plasma devices and in space physics is an important endeavor [1–3]. The basis for numerous numerical models is the collisionless linear Vlasov equation with specified electromagnetic wave fields or from a self-consistent treatment of the nonlinear Vlasov–Maxwell equations [4,5]. There is a long history of the use of an expansion of the space and velocity dependent ion distribution function in Fourier–Hermite basis functions [6–14]. The choice of a Fourier expansion in the spatial variable is justified by the use of a finite domain and periodic boundary conditions. Hermite polynomials are a logical choice for the basis set in velocity as the cartesian velocity components are on the infinite interval and the Hermite polynomials are orthogonal with the Maxwellian weight function. Hermite polynomial expansions are also employed in other applications [15,16]. However, several authors have reported convergence problems with this approach due to two phenomena referred to as "filamentation" [7–9,17] and "recurrence" [7,10,11,18]. They both arise from the free-streaming convective term in the Vlasov equation and the limited resolution of the distribution function owing to the finite discretizations employed to solve the Vlasov equation.

It has been customary in numerous applications of the Vlasov equation to consider an oscillatory perturbation of the velocity distribution function in space of the form $\cos(\tilde{k}\tilde{x})$. If only the collisionless free-streaming term is retained, the solution evolves along the characteristic $\tilde{x} \to \tilde{x} - \tilde{v}\tilde{t}$ and the exact solution is of the form $\cos[\tilde{k}(\tilde{x} - \tilde{v}\tilde{t})]$ as discussed in Section 2. The velocity distribution will thus oscillate in velocity and the frequency of the oscillations will increase with time. The numerical challenge posed by this problem is to resolve the rapid

* Corresponding author. Address: Department of Chemistry, University of British Columbia, 2036 Main Mall, Vancouver, BC, Canada V6T 1Z1. Tel.: +1 604 822 3997.
*E-mail address:* shizgal@chem.ubc.ca (B.D. Shizgal).

0021-9991/$ - see front matter 
doi:10.1016/j.jcp.2006.06.017

oscillations of the distribution function in velocity space especially for long times. If some grid is chosen on which the Vlasov equation is solved, the resolution of the grid must be made sufficiently fine in order to accurately resolve the distribution function. The same issue arises if the distribution function is expanded in some basis set such as the Hermite functions. The number of terms in the expansion must increase in order to provide the resolution needed to accurately approximate the distribution function. It is these rapid oscillations of the distribution function that are referred to as fine structures or filamentation [7–9,17]. It is also related to the non-physical recurrence of the initial data in several simulations that have been reported [7,10,11,18].

In the present paper, we employ a Fourier–Hermite expansion to represent the velocity distribution function in position and velocity as done previously [6–12,14]. The Fourier–Hermite coefficients in this expansion satisfy a set of ordinary differential equations in time determined from the Vlasov equation. Owing to the nature of the initial perturbation chosen, only three Fourier modes are required for an exact representation of the distribution function in position. By contrast, the infinite series in the Hermite basis functions must be truncated at some finite number, $N$. It has been demonstrated [6,9,10,12] that this truncation leads to what appears to be an instability and instead a closure condition which relates the $(N+1)$st expansion coefficient (or moment) to the lower order moments is required [9]. An interpretation of the different closure conditions in terms of the eigenvalue spectrum of the discretized free streaming operator in the Vlasov equation has been presented by Joyce et al. [9] and by Holloway [13].

The main objective of the present paper is to demonstrate spectral convergence of the Hermite expansion of the distribution function. We compare the exact solution with the distribution function determined from the time integration of the set of ordinary differential equations for the expansion coefficients with and without a closure condition. The exact Hermite expansion coefficients are also calculated from the exact analytic solution and spectral convergence is demonstrated. We also include an important scaling of the Hermite basis functions [14–16,19] and show the improved convergence that can be achieved. In Section 2, the solution of the free streaming term of the Vlasov equation is presented for periodic boundary conditions. The solution given by the Fourier–Hermite expansion is discussed in Section 3. The exact representation in the Fourier–Hermite basis is calculated in Section 4. A discussion of the results and spectral convergence is presented in Section 5.

## 2. The Vlasov equation

The linear collisionless Vlasov equation for the interaction of an ensemble of ions, of charge $q$ and mass $m$, with a uniform magnetic field $\mathbf{B} = B_0\hat{\mathbf{e}}_\mathbf{z}$ directed along the $z$-axis and a perpendicular electric field $\mathbf{E}(\tilde{x},\tilde{t}) = E_0(\tilde{x},\tilde{t})\hat{\mathbf{e}}_\mathbf{x}$ is given by the Vlasov equation

$$\frac{\partial \tilde{f}}{\partial \tilde{t}} + \tilde{v}_x\frac{\partial \tilde{f}}{\partial \tilde{x}} + \frac{q}{m}\left[B_0\tilde{v}_y + E_0(\tilde{x},\tilde{t})\right]\frac{\partial \tilde{f}}{\partial \tilde{v}_x} - \frac{q}{m}B_0\tilde{v}_x\frac{\partial \tilde{f}}{\partial \tilde{v}_y} = 0. \tag{1}$$

An often used technique to solve Eq. (1) is to expand the ion distribution function in a Fourier series in space and Hermite polynomials in velocity. A set of coupled ordinary differential equations for the expansion coefficients is thus obtained and integrated in time. The time integration of these moment equations yields numerical instabilities. These instabilities arise from the convective term and in this note we address this aspect of the spectral solution. Hence, we consider the solution of the simplified Vlasov equation with only the convective term and deletion of the terms with the electromagnetic fields, that is

$$\frac{\partial \tilde{f}}{\partial \tilde{t}} + \tilde{v}_x\frac{\partial \tilde{f}}{\partial \tilde{x}} = 0 \tag{2}$$

with the initial condition

$$\tilde{f}(\tilde{x},\tilde{v}_x,0) = \widetilde{F}(\tilde{v}_x)\left\{1+\cos(\tilde{k}\tilde{x})\right\}, \tag{3}$$

where $\widetilde{F}$ is the Maxwellian distribution function

$$\widetilde{F}(\tilde{v}_x) = \sqrt{\frac{m}{2\pi k_\mathrm{B}\widetilde{T}}}\exp\left[-\frac{m\tilde{v}_x^2}{2k_\mathrm{B}\widetilde{T}}\right], \tag{4}$$

and $k_B$ is the Boltzmann constant and $\widetilde{T}$ is the ion temperature. Eq. (3) is often chosen as the initial perturbation from Maxwellian in the study of Landau damping for the Vlasov–Poisson equations.

Given that the initial condition is periodic of period $2\pi/\tilde{k}$, we solve Eq. (2) on the domain $[-\pi/\tilde{k}, \pi/\tilde{k}]$ with periodic boundary conditions. We define the dimensionless variables

$$x = \tilde{k}\tilde{x}, \quad v = \sqrt{\frac{m}{k_B\widetilde{T}}}\tilde{v}_x, \quad t = \tilde{k}\sqrt{\frac{k_B\widetilde{T}}{m}}\tilde{t}, \quad f = \tilde{k}\sqrt{\frac{k_B\widetilde{T}}{m}}\tilde{f}, \tag{5}$$

and rewrite Eqs. (2) and (3) in the dimensionless form

$$\frac{\partial f}{\partial t} + v\frac{\partial f}{\partial x} = 0, \quad x \in [-\pi, \pi] \tag{6}$$

and

$$f(x, v, 0) = \frac{1}{\sqrt{2\pi}} \exp\left[-\frac{v^2}{2}\right](1 + \cos x). \tag{7}$$

The analytic solution of Eq. (6) satisfying the initial condition (7) is

$$f(x, v, t) = \frac{1}{\sqrt{2\pi}} \exp\left[-\frac{v^2}{2}\right]\{1 + \cos(x - vt)\}. \tag{8}$$

## 3. Fourier–Hermite solution of the Vlasov equation

We expand the ion velocity distribution function in the Fourier–Hermite basis, that is

$$f(x, v, t) = \sum_{l=-1}^{1}\sum_{n=0}^{\infty}(-\mathrm{i})^n \hat{g}_{l,n}(t)F_l(x)h_n(sv), \tag{9}$$

where $F_l(x)$ and $h_n(sv)$ are the Fourier and Hermite basis functions, respectively, $s$ is an important scaling factor [14–16,19] and $\mathrm{i} = \sqrt{-1}$. The Fourier basis functions are $F_l(x) = \mathrm{e}^{\mathrm{i}xl}$ and satisfy the orthogonality condition $\frac{1}{2\pi}\int_{-\pi}^{\pi} F_l F_{l'}^* \,\mathrm{d}x = \delta_{l,l'}$ where the asterisk denotes the complex conjugate. In view of the form of the analytic solution, Eq. (8) in the present application, the sum over Fourier modes is truncated at $l = \pm 1$. If $H_n(x)$ denotes the Hermite polynomials given by

$$H_n(x) = (-1)^n \mathrm{e}^{x^2}\left(\frac{\mathrm{d}}{\mathrm{d}x}\right)^n \mathrm{e}^{-x^2}, \tag{10}$$

the Hermite basis functions, $h_n$, are defined by

$$h_n(x) = \frac{H_n(x)}{\pi^{1/4}\sqrt{2^n n!}} \exp\left[-\frac{x^2}{2}\right], \tag{11}$$

and satisfy the orthogonality condition

$$\int_{-\infty}^{\infty} h_n h_{n'} \,\mathrm{d}x = \delta_{n,n'}. \tag{12}$$

We use the expansion (9) in Eq. (6), multiply the equation by $F_{l'}h_{n'}$ and integrate over position and velocity, and we get

$$\frac{\mathrm{d}\hat{g}_{l,n}}{\mathrm{d}t} + \frac{l}{s}\left(\sqrt{\frac{n}{2}}\hat{g}_{l,n-1} - \sqrt{\frac{n+1}{2}}\hat{g}_{l,n+1}\right) = 0, \qquad l = -1, 0, 1; \quad n = 0, \ldots, \infty. \tag{13}$$

In obtaining Eq. (13), we used the orthogonality conditions for the Fourier–Hermite basis functions and the recurrence relation

$$xh_n(x) = \sqrt{\frac{n}{2}}h_{n-1}(x) + \sqrt{\frac{n+1}{2}}h_{n+1}(x). \tag{14}$$

Given that the initial condition for Eq. (13) is real, the coefficients $\hat{g}_{l,n}$ remain real for all time [9]. Also, since the distribution function is real, we have that $\hat{g}_{-l,n} = \hat{g}_{l,n}$.

The moment equations, Eq. (13), define the time evolution of the matrix of Fourier–Hermite coefficients. This set of coupled equations forms an infinite hierarchy which must be truncated in some reasonable manner, i.e.

$$\frac{\mathrm{d}g_{l,n}}{\mathrm{d}t} + \frac{l}{s}\left(\sqrt{\frac{n}{2}}g_{l,n-1} - \sqrt{\frac{n+1}{2}}g_{l,n+1}\right) = 0, \qquad l = -1, 0, 1; \quad n = 0, \ldots, N. \tag{15}$$

The expansion coefficients so computed, $g_{l,n}$, are approximations to the exact ones, $\hat{g}_{l,n}$. The truncation of the moment equations for this simplified Vlasov equation as well as for the Vlasov–Poisson system has received considerable attention in the literature. We show, as discussed previously [6–10,12], that the truncation condition usually adopted

$$g_{l,n} = 0 \qquad n \geqslant N+1 \tag{16}$$

results in large oscillations in the distribution function and is not useful. These instabilities arise because the time derivative of $g_{l,N}$, given by Eq. (15), requires $g_{l,N+1}$ which is discarded. There have been numerous analyses of this problem and remedies that include filtering [7,18,17], addition of a collision term that acts as a damping term [8–10], and a closure condition based on interpolation so that the moment $g_{l,N+1}$ that occurs in Eq. (15) is not discarded [9]. So instead of (16), we employ an estimate of the value of $g_{l,N+1}$ with an extrapolation from lower order moments. One such scheme is based on the fourth order interpolation [9]

$$g_{l,N+1} = 4g_{l,N} - 6g_{l,N-1} + 4g_{l,N-2} - g_{l,N-3}. \tag{17}$$

This method of truncation with interpolation is adopted in the numerical solution of the Vlasov equation in order to avoid the recurrence effect [9,10]. Joyce et al. [9] and Holloway [13] have shown that the truncation, Eq. (16), reduces the otherwise continuous eigenvalue spectrum of the infinite set of equations, Eq. (13), to a discrete spectrum of purely imaginary eigenvalues. Thus the solution of Eq. (15) with Eq. (16) is oscillatory. By contrast, the use of the interpolation, Eq. (17), introduces a real part to the eigenvalues and hence the system, Eq. (15), with Eq. (17) exhibits dissipation. We have confirmed these behaviors numerically.

## 4. Expansion of the analytic solution in Hermite polynomials

The exact expansion coefficients are given by

$$\hat{g}_{l,n}(t) = \frac{\mathrm{i}^n}{2\pi}\int_{-\pi}^{\pi}\int_{-\infty}^{\infty} f(x,v,t)F_l(x)h_n(sv)\,\mathrm{d}x\,\mathrm{d}v. \tag{18}$$

In view of the form of the solution Eq. (8), only the coefficients with $l = 0$ and $l = \pm 1$ are nonzero. The main objective reduces to a study of the convergence of the expansions of $F(v)\cos(vt)$ and $F(v)\sin(vt)$ in Hermite basis functions. This is similar to a study reported by Tang [15] who employed Gaussian quadratures to calculate the expansion coefficients. In this paper we make use of exact results [20] for the integrals that occur. These are

$$\int_{-\infty}^{\infty}\mathrm{d}y\,\exp[-a^2y^2]\cos(by)H_{2n}(y) = \sqrt{\pi}\exp\left[-\left(\frac{b}{2a}\right)^2\right]\frac{1}{a}\left(\frac{a^2-1}{a^2}\right)^n H_{2n}\left[\frac{b}{2a(1-a^2)^{1/2}}\right], \tag{19}$$

$$\int_{-\infty}^{\infty}\mathrm{d}y\,\exp[-a^2y^2]\sin(by)H_{2n+1}(y) = \mathrm{i}\sqrt{\pi}\exp\left[-\left(\frac{b}{2a}\right)^2\right]\frac{a^2-1}{|a^2-1|}\frac{(a^2-1)^{1/2}}{a^2}\left(\frac{a^2-1}{a^2}\right)^n H_{2n+1}\left[\frac{b}{2a(1-a^2)^{1/2}}\right], \tag{20}$$

for $a \neq 1$, and

$$\int_{-\infty}^{\infty} \mathrm{d}y \exp[-y^2]\cos(by)H_{2n}(y) = (-1)^n\sqrt{\pi}b^{2n}\exp\left[-\frac{b^2}{4}\right], \tag{21}$$

$$\int_{-\infty}^{\infty} \mathrm{d}y \exp[-y^2]\sin(by)H_{2n+1}(y) = (-1)^n\sqrt{\pi}b^{2n+1}\exp\left[-\frac{b^2}{4}\right], \tag{22}$$

for $a = 1$. The nonzero coefficients defined by Eq. (18) are given by

$$\hat{g}_{0,2n} = \frac{1}{\pi^{1/4}}\frac{(-1)^n[(2n)!]^{1/2}}{2^n n!}\frac{s}{(s^2+1)^{1/2}}\left[\frac{s^2-1}{s^2+1}\right]^n, \tag{23}$$

and for $s \neq 1$

$$\hat{g}_{1,2n}(t) = \frac{1}{\pi^{1/4}}\frac{(-1)^n}{2^{n+1}[(2n)!]^{1/2}}\exp\left[-\frac{t^2}{2(1+s^2)}\right]\frac{s}{(1+s^2)^{1/2}}\left[\frac{1-s^2}{1+s^2}\right]^n H_{2n}\left[\frac{st}{(s^4-1)^{1/2}}\right], \tag{24}$$

$$\hat{g}_{1,2n+1}(t) = \frac{1}{(2\pi^{1/2})^{1/2}}\frac{\mathrm{i}^{2n+1}}{2^{n+1}[(2n+1)!]^{1/2}}\exp\left[-\frac{t^2}{2(1+s^2)}\right]\frac{1-s^2}{|s^2-1|}\frac{s(1-s^2)^{1/2}}{1+s^2}\left[\frac{1-s^2}{1+s^2}\right]^n H_{2n+1}\left[\frac{st}{(s^4-1)^{1/2}}\right], \tag{25}$$

whereas for $s = 1$

$$\hat{g}_{1,2n}(t) = \frac{1}{(2\pi^{1/2})^{1/2}}\frac{1}{2^{n+1}[(2n)!]^{1/2}}t^{2n}\exp\left[-\frac{t^2}{4}\right], \tag{26}$$

$$\hat{g}_{1,2n+1}(t) = \frac{1}{\pi^{1/4}}\frac{1}{2^{n+2}[(2n+1)!]^{1/2}}t^{2n+1}\exp\left[-\frac{t^2}{4}\right]. \tag{27}$$

These results permit a careful study of the spectral convergence of the exact solution as well as the solution obtained from the time integration of the moment equations, Eq. (15), with the truncation condition given by Eq. (16) or Eq. (17). We also study the role of scaling parameter, $s$, on the rate of convergence.

## 5. Discussion of results: spectral convergence

The main objective of the present note is twofold. We are primarily interested in the behavior of the moment equations, Eq. (15), with regards to the numerical stability of the time integration for long times. We study the role of the scaling parameter in accelerating the convergence and the closure of the moment equations with an interpolation scheme, Eq. (17). We also study the spectral convergence of the exact expansion as this provides limits on the applicability of the Hermite basis function expansion. The coefficients $g_{0,n}$ do not depend on time, so we will consider only the coefficients $g_{1,n}$. A fourth-order Runge–Kutta ODE solver was employed to integrate Eq. (15). We have confirmed numerically that the eigenvalues of this system with the truncation equation (16) and the interpolation equation (17) lie inside the stability region of this ODE solver. The features of the solution of the free streaming portion of the Vlasov equation that we report are not due to the ODE solver used.

Fig. 1 shows a comparison of the variation of the exact coefficients (solid line), obtained from Eqs. (23), (26) and (27), and their approximation from the integration of Eq. (15) (solid circles) with no scaling ($s = 1$) and with truncation of the moment equations at $N = 50$. For the smaller times chosen in Fig. 1a and b, the two results are almost indistinguishable. However, it is clear from the results for $t = 10$ in Fig. 1d that an instability has occurred in the numerical integration of the moment equations. The instability is also apparent in Fig. 1c for large $n$. One reason is that spurious oscillations are excited at the boundary, $n = N$, and then propagate back to smaller $n$ [12]. Moreover for $t = 10$, the coefficients are increasing with $n$ and it is clear that the expansion of the solution in Hermite polynomials requires additional terms to achieve convergence. The variation of the distribution at $x = 0$ versus $v$ is shown in Fig 2 for the conditions in Fig. 1. The incomplete convergence of the distribution at the extremes of the domain shown for $t = 8$ and 10 in Fig. 2c and d, respectively, is clear.

In Fig. 3, we show a dramatic improvement in these results with the scaling of the Hermite polynomials ($s = 1.25$). The most notable feature of the results in Fig. 3 is that the variation of the expansion coefficients

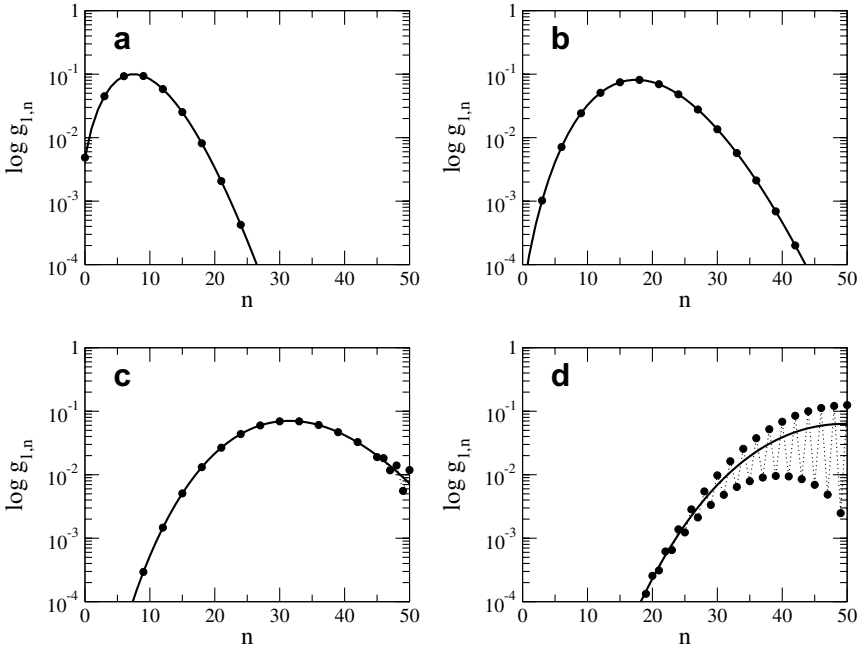


Fig. 1. Variation of the coefficients $g_{1,n}$ versus $n$ for $t$ equal to: (a) 4, (b) 6, (c) 8 and (d) 10. Solid lines represent the analytic results derived from Eqs. (23), (26) and (27); solid circles are the results from the numerical integration of Eq. (15); $N = 50$, $s = 1.0$; truncation condition, Eq. (16), employed.

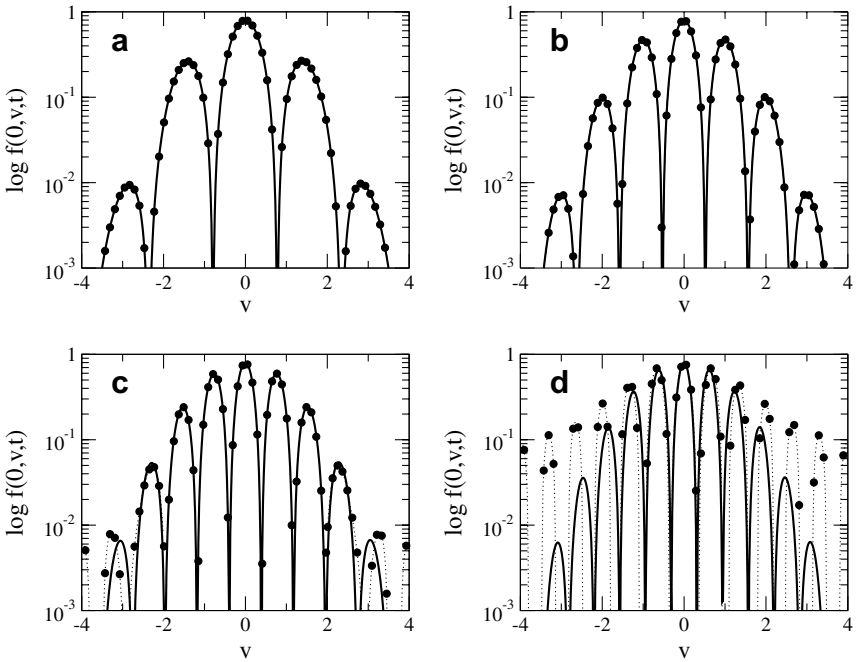


Fig. 2. Variation of the distribution function versus velocity at $x = 0$ for $t$ equal to: (a) 4, (b) 6, (c) 8 and (d) 10. Solid lines represent the analytical solution, Eq. (8); solid circles are the results from the numerical integration of Eq. (15); $N = 50$, $s = 1.0$; truncation condition, Eq. (16), employed.

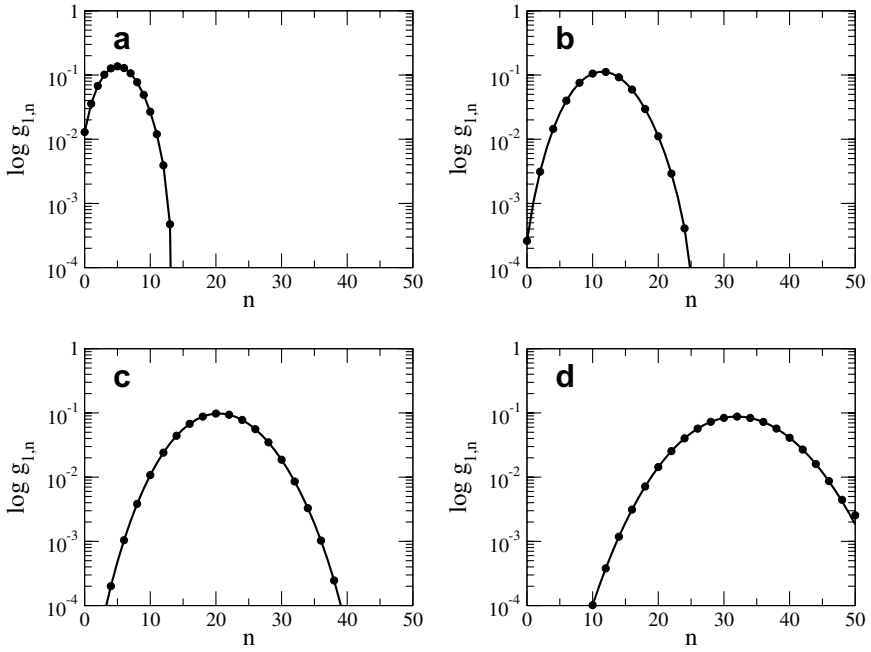


Fig. 3. Variation of the coefficients $g_{1,n}$ versus $n$ for $t$ equal to: (a) 4, (b) 6, (c) 8 and (d) 10. Solid lines represent the analytic results derived from Eqs. (23)–(25); solid circles are the results from the numerical integration of Eq. (15); $N = 50$, $s = 1.25$; truncation condition, Eq. (16), employed.

has been displaced to lower $n$ for all times and it is clear that the convergence of the expansion in Hermite basis functions is more rapid than in Fig. 1 with $s = 1$. The curve for $t = 10$ has attained a maximum at about $n \approx 30$ and then decreases whereas the corresponding curve in Fig. 1 has not achieved a maximum by $n = 50$. The coefficients $g_{1,n}$ are indistinguishable from the exact coefficients, $\hat{g}_{1,n}$, except for $t = 10$ and $n \sim 50$ in Fig. 3d. The value of $s$ used lies in the middle of the range of values employed in the partial optimization of $s$ as discussed in Fig. 9 later.

In Fig. 4, we show analogous results for $s = 1$ and with the application of the interpolation closure given by Eq. (17). The important feature is that the instability shown in Fig. 1 for $t = 10$ does not occur but the variation versus $n$ has not changed which is not unexpected. The convergence in Hermite polynomials remains restricted by the finite number of terms retained and the importance of appropriately scaling the Hermite polynomials is clear. The variation of the distribution function versus velocity at $x = 0$ for two reduced times $t = 8$, 10, is shown in Fig. 5a and b, for the conditions of Fig. 1 ($s = 1.25$ and without interpolation), and in Fig. 5c and d for the conditions of Fig. 4 ($s = 1$ and with interpolation). The results with scaling provide the best solutions.

Filamentation and recurrence phenomena can be easily explained in terms of the time evolution of the coefficients $g_{1,n}$. As previously discussed, filamentation refers to the oscillations of the distribution function versus velocity with a frequency that increases with time as shown in Figs. 2 and 5. It is a physical consequence of the free-streaming evolution that results in the variation of the expansion coefficients being displaced to larger $n$ as time increases (solid line in Fig. 1). The convergence of the expansion in Hermite basis functions is thus slower. Fig. 6 compares the variation of $g_{1,n}$ versus $n$ for truncation, Eq. (16) and interpolation, Eq. (17), for a small time interval $t = 9$ to $t = 11.5$ and illustrates the nonphysical recurrence effect. As shown in Fig. 6a ($t = 9$) the coefficients $g_{1,n}$ computed using the truncation condition (16), represented by solid circles and dashed lines, are almost the same as the ones computed using the interpolation condition (17), represented by the solid lines, except for small oscillations for $n \approx N$. However, for the larger times chosen, the time evolution is different. The interpolation condition (17) preserves the main feature of the free-streaming evolution, that is, the variation of the coefficients is progressively displaced to greater $n$. With the truncation condition (16), the variation of the

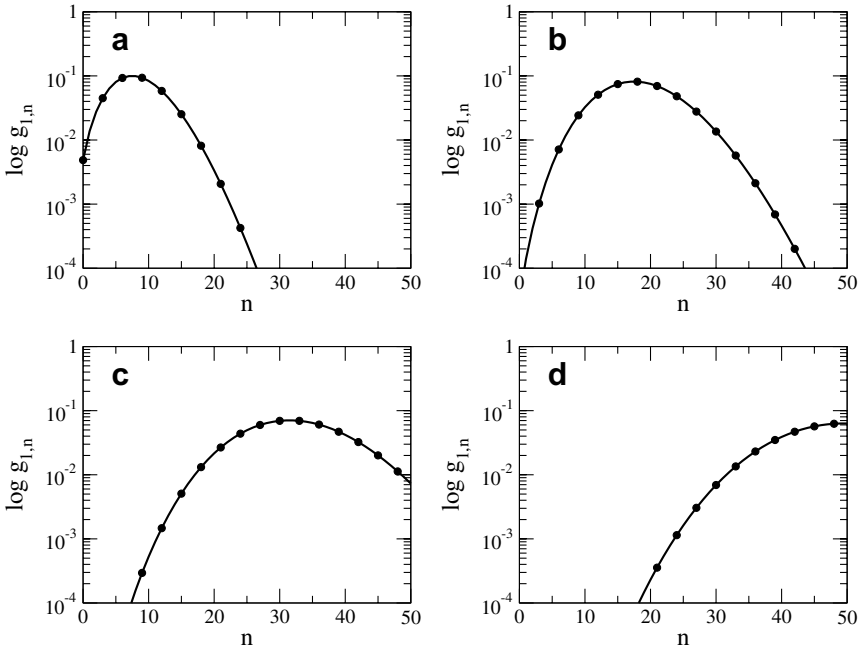


Fig. 4. Variation of the coefficients $g_{1,n}$ versus $n$ for $t$ equal to: (a) 4, (b) 6, (c) 8 and (d) 10. Solid lines represent the analytic results derived from Eqs. (23), (26) and (27); solid circles are the results from the numerical integration of Eq. (15); $N = 50$, $s = 1.0$; $g_{1,N+1} = 4g_{1,N} - 6g_{1,N-1} + 4g_{1,N-2} - g_{1,N-3}$, Eq. (17).

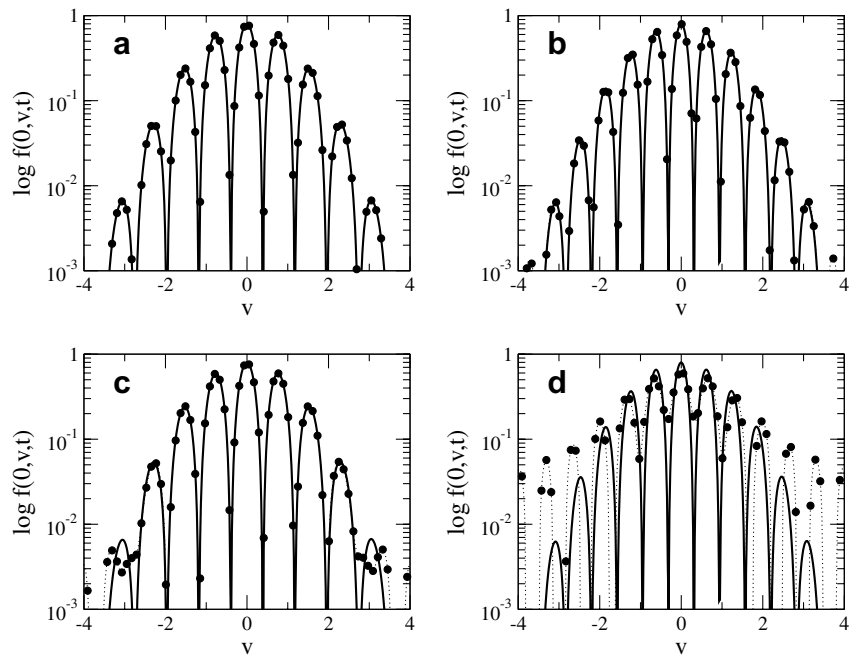


Fig. 5. Variation of the distribution function versus velocity at $x = 0$ and $N = 50$. Solid lines represent the analytic solution, Eq. (8); solid circles and dashed lines are the results from the numerical integration of Eq. (15) for $g_{1,N+1} = 0$ and $s = 1.25$ at the reduced time $t$ equal to (a) 8 and (b) 10, and for $g_{1,N+1} = 4g_{1,N} - 6g_{1,N-1} + 4g_{1,N-2} - g_{1,N-3}$ and $s = 1$ at the reduced time $t$ equal to (c) 8 and (d) 10.

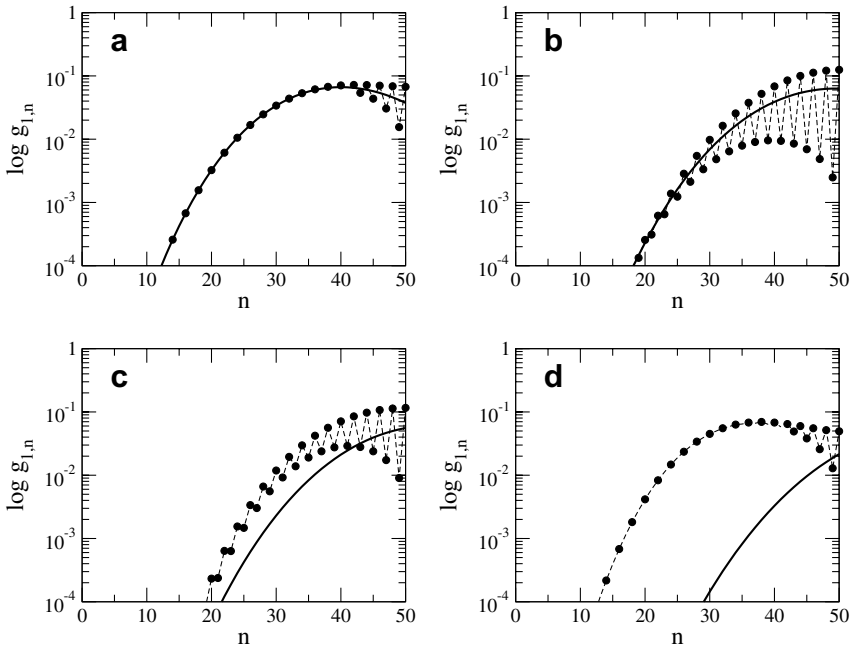


Fig. 6. Variation of the coefficients $g_{1,n}$ versus $n$ for $t$ equal to: (a) 9, (b) 10, (c) 10.5 and (d) 11.5. Solid circles and dashed lines represent the results from the numerical integration of Eq. (15) with the truncation condition $g_{1,N+1} = 0$; solid lines represent the results from the numerical integration of Eq. (15) with interpolation closure $g_{1,N+1} = 4g_{1,N} - 6g_{1,N-1} + 4g_{1,N-2} - g_{1,N-3}$.

coefficients $g_{1,n}$ is reflected back in time as seen clearly in Fig. 6c ($t = 10.5$) and for $t = 11.5$, Fig. 6d, it is almost the same as at $t = 9$, Fig. 6a. Thus the computed distribution function appears to be a periodic function of time arising from the truncation condition (16).

In order to study the spectral convergence of the exact expansion, we compare the exact solution, Eq. (8), with the solution computed using the first $N$ exact Hermite coefficients, given by Eqs. (23)–(25) for $s \neq 1$ or Eqs. (23), (26) and (27) for $s = 1$. We define the local truncation error as

$$\mathrm{TE}_N(x,v,t) = \log\left| f(x,v,t) - \sum_{l=-1}^{1}\sum_{n=0}^{N}(-1)^n \hat{g}_{l,n}(t) F_l(x) h_n(sv)\right|, \tag{28}$$

and consider the local truncation error at $x = 0$.

Fig. 7 shows the local truncation error, Eq. (28), versus $v$ for a fixed number of Hermite polynomials, $N = 50$, at three reduced times $t = 8$, 10 and 12 and for (a) $s = 1$ and (b) $s = 1.5$. The errors increase with time and appear to attain a maximum value in the vicinity of $v = 0$. In Fig. 8, we show for $t = 12$ the decrease in $\mathrm{TE}_N(x = 0, v, t = 12)$ for $N = 50$, 75 and 100 for (a) $s = 1$ and (b) $s = 1.5$. The improvement in the convergence is evident with the appropriate scaling. As in Fig. 7, the error in the vicinity of $v = 0$ appears to be a maximum.

In order to define an optimum value for the scaling parameter, we define the $L^{(N)}_{\max}$ error

$$L^{(N)}_{\max}(x,t) = \max_{v_1 \leqslant v \leqslant v_2} \mathrm{TE}_N(x,v,t), \tag{29}$$

where $v_1$ and $v_2$ define the velocity domain considered. We chose $v_1 = -10$ and $v_2 = 10$.

Fig. 9 shows the $L^{(N)}_{\max}$ error, Eq. (29), versus $N$ for $x = 0$ at the reduced time $t = 12$ for different values of the scaling parameter. It is clear that the results are not improved for $s = 0.75$ (solid line a). However, for $s > 1$, the $L^{(N)}_{\max}$ error is dramatically reduced. The optimum value of the scaling parameter appears to be $s = 1.5$ (solid line d). The $L^{(N)}_{\max}$ error with $s = 1.75$ (solid line e) is in fact greater than for $s = 1.5$ (solid line d) for $N > 60$. It is important to stress that these conclusions depend on the time chosen. If we had considered a different reduced time, the optimum value of the scaling parameter would be different.

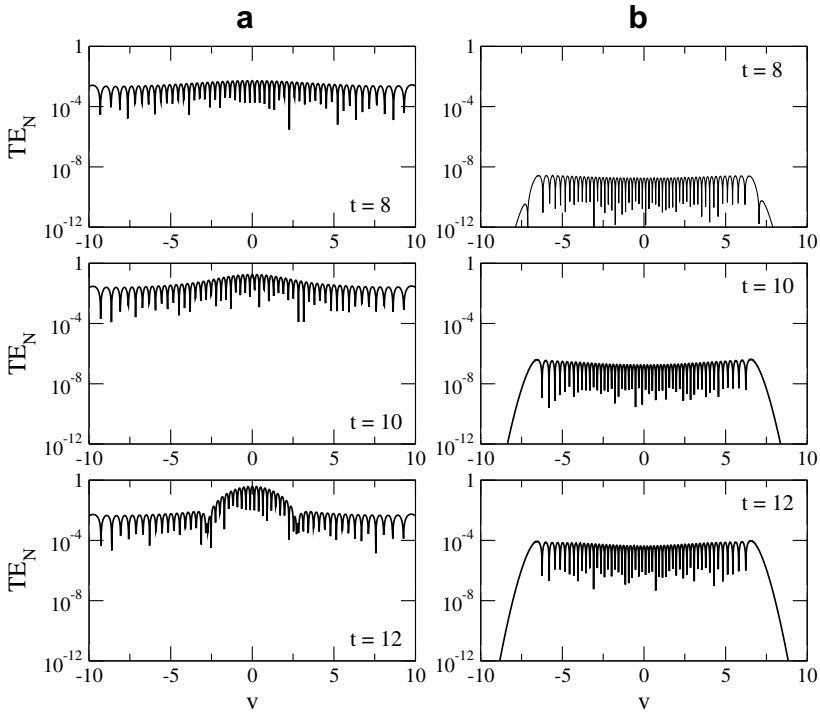


Fig. 7. Local truncation error at $x = 0$ for a fixed number of Hermite polynomials, $N = 50$; (a) $s = 1$ and (b) $s = 1.5$.

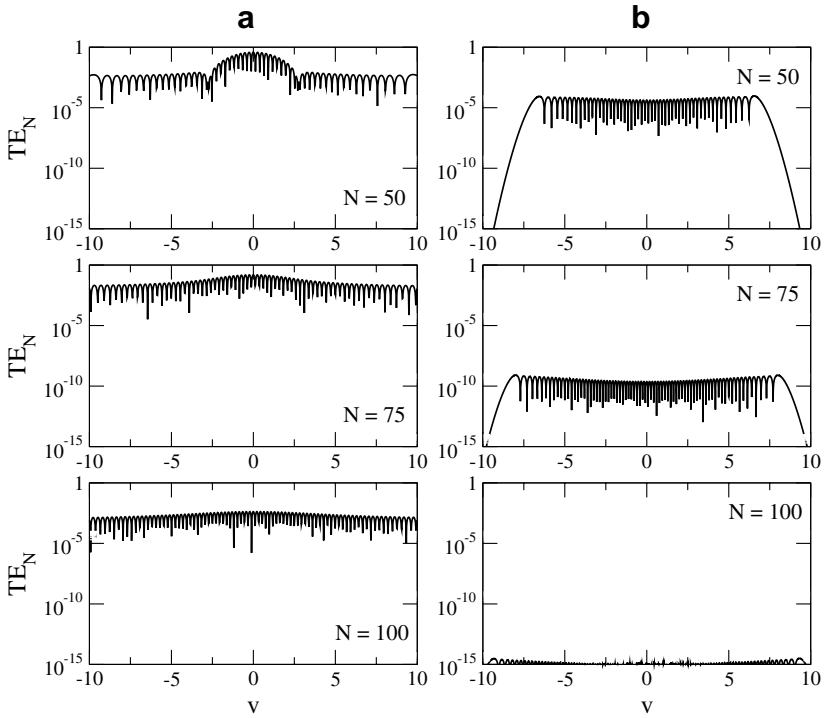


Fig. 8. Local truncation error at $x = 0$ at the reduced time $t = 12$; (a) $s = 1$ and (b) $s = 1.5$.

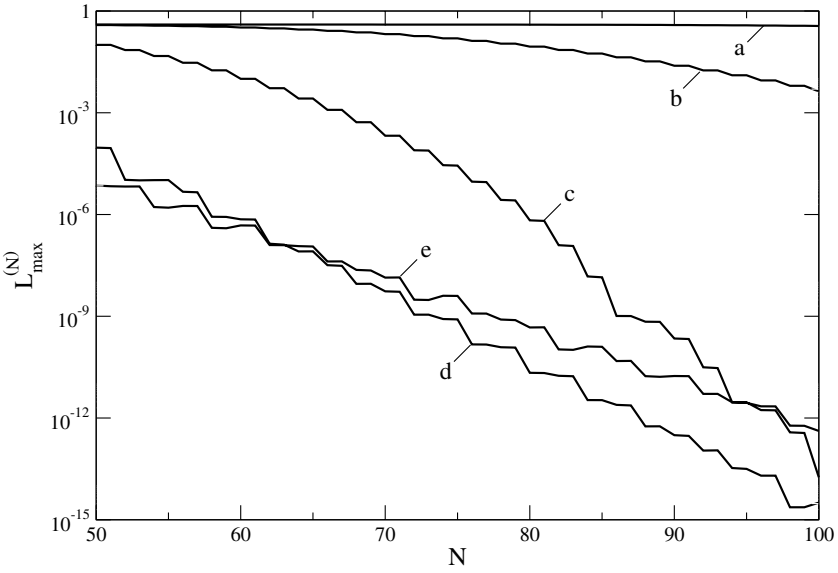


Fig. 9. $L_{\max}^{(N)}$ error at $x = 0$ versus number of Hermite polynomials at the reduced time $t = 12$ for the scaling parameter equal to: (a) 0.75, (b) 1.0, (c) 1.25, (d) 1.5 and (e) 1.75.

## Acknowledgements

This research is funded by a grant to B.D.S. and Dr. Andrew Yau of the University of Calgary from the Natural Sciences and Engineering Research Council (NSERC) of Canada and the Canadian Space Agency. B.D.S. is very grateful to Dr. H. Hayakawa and Dr. T. Mukai for their hospitality at the Institute of Space and Astronautical Science, Japan, where the major part of this work was carried out.

## References

[1] R. Spektor, E.Y. Choueiri, Ion acceleration by beating electrostatic waves: domain of allowed acceleration, Phys. Rev. E 69 (2004) 046402.
[2] A.K. Ram, A. Bers, D. Benisti, Ionospheric ion acceleration by multiple electrostatic waves, J. Geophys. Res. 103 (1998) 9431–9440.
[3] G.B. Crew, T.S. Chang, Asymptotic theory of ion conic distributions, Phys. Fluids 28 (1985) 2382–2394.
[4] T.H. Stix, Waves in Plasmas, AIP, New York, 1992.
[5] F. Valentini, P. Veltri, A. Mangeney, A numerical scheme for the integration of the Vlasov–Poisson system of equations in the magnetized case, J. Comput. Phys. 210 (2005) 730–751.
[6] T.P. Armstrong, Numerical studies of the nonlinear Vlasov equation, Phys. Fluids 10 (1967) 1269–1280.
[7] C.Z. Cheng, B. Knorr, The integration of the Vlasov equation in configuration space, J. Comput. Phys. 22 (1976) 330–351.
[8] F.C. Grant, M.R. Feix, Fourier–Hermite solutions of the Vlasov equations in the linearized limit, Phys. Fluids 10 (1967) 696–702.
[9] G. Joyce, G. Knorr, H.K. Meier, Numerical integration methods of the Vlasov equation, J. Comput. Phys. 8 (1971) 53–63.
[10] G. Knorr, M. Shoucri, Plasma simulation as eigenvalue problem, J. Comput. Phys. 14 (1974) 1–7.
[11] J. Canosa, J. Gazdag, J.E. Fromm, The recurrence of the initial state in the numerical solution of the Vlasov equation, J. Comput. Phys. 15 (1974) 34–45.
[12] G.W. Hammett, M.A. Beer, W. Dorland, S.C. Cowley, S.A. Smith, Developments of the gyrofluid approach to tokamak turbulence simulations, Plasma Phys. Control. Fusion 35 (1993) 973–985.
[13] J.P. Holloway, Spectral velocitiy discretizations for the Vlasov–Maxwell equations, Trans. Theory Stat. Phys. 25 (1996) 1–32.
[14] J.W. Schumer, J.P. Holloway, Vlasov simulations using velocity-scaled Hermite representations, J. Comput. Phys. 144 (1998) 626–661.
[15] T. Tang, The Hermite spectral method for Gaussian-type functions, SIAM J. Sci. Comput. 14 (1993) 594–606.
[16] K.L. Tse, J.R. Chasnov, A Fourier–Hermite pseudospectral method of penetrative convection, J. Comput. Phys. 142 (1998) 489–505.
[17] H. Figua, F. Bouchut, M.R. Feix, E. Fijalkow, Instability of the filtering method for Vlasov's equation, J. Comput. Phys. 159 (2000) 440–447.
[18] A.J. Klimas, A method for overcoming the velocity space filamentation problem in collisionless plasma model solutions, J. Comput. Phys. 68 (1987) 202–226.

[19] B. Shizgal, D.R.A. McMahon, Electric field dependence of transient electron transport properties in rare-gas moderators, Phys. Rev. A 32 (1985) 3669–3690.
[20] A.P. Prudnikov, Y.A. Brychkov, O.I. MarichIntegral and Series, vol. 3, Gordon & Breach, New York, 1986.